RESEARCH PAPER

Nanostructured Tin Sulfide Thin Films: Preparation via Chemical Bath Deposition and Characterization

Rusul A.Ghazi[1], Alaa Jabbar Ghazai[2], Zina Mahmood Shaban[3], Khalid Haneen Abass[4], Nadir Fadhil Habubi[3], Sami Salman Chiad[3,*]

[1]Department of Medical Physics, Al–Mustaqbal University College, , Babylon, Iraq

[2] Department of Physics, College of Science, Al-Nahrain University, Iraq

[3]Department of Physics, College of Education, Mustansiriyah University, Iraq

[4]Department of Physics, College of Education for Pure Sciences, University of Babylon, Iraq

ARTICLE INFO

Article History:
Received 08 October 2020
Accepted 18 December 2020
Published 01 January 2021

Keywords:
AFM
Band gap
CBD
Optical properties
SnS thin film
XRD

ABSTRACT

Nanostructured tin sulfide (SnS) films were grown by chemical bath deposition (CBD) employing trisodium citrate (TSC) as complex agent. Investigation of the effect of different molar concentrations of TSC (0.10, 0.15 and 0.20 M) on the phases of SnS was done. Structure, morphology and optical properties were studied through the use of x-ray diffraction XRD, which proves that the as-prepared SnS films orthorhombic polycrystalline structure. XRD displays that peak of maximum intensity corresponds to the preferred orientation (002) of SnS films at TSC concentration 0.20 M. The decrement of average crystalline size values was due increment of TSC content. A study of SnS morphology indicates the presence of homogeneous grains, while when concentration of TSC of 0.20 M, the grains were not homogeneous and have different sizes. The AFM image showed that the grain size was observed in the area of 72.57 nm to 60.35 nm with concentration of TSC from 0.10 M to 0.20 M respectively. The results showed excellent optical transparency. The optical transmittance reduced from 95 to 80% with increasing TSC content. The ban gap was also reduced of 1.45 to 1.25 eV with increasing TSC content. The results refer that TCS act as a crucial role in the grown of SnS films.

How to cite this article
Ghazi R.A., Ghazai A.J., Shaban Z.M., Abass Kh.H, Habubi N.F., Chiad S.S. Nanostructured Tin Sulfide Thin Films: Preparation via Chemical Bath Deposition and Characterization. J Nanostruct, 2021; 11(1): 66-72. DOI: 10.22052/JNS.2021.01.008

INTRODUCTION

A thin film is a material layer with a thickness ranging from fractions of a nanometer (monolayer) to several micrometers [1-5]. The method of "deposition" is used to make thin films. Deposition is a thin film coating technique that involves changing the four states of matter: solid, liquid, vapor, and plasma [6-9]. Any deposition process aims to produce thin films that are repeatable, controlled, and predictable [10]. Large area thin films must be deposited using chemical processes due to factors of simplicity, affordability, and input energy. Chemical methods for the development of thin films include electrodeposition, electroconversion, electrophoresis, electroless, spray pyrolysis, dip growth, and chemical deposition [11-15]. Thin films are used in a wide range of applications, from nanostructures in nano electronics to multi-square-meter coatings on window glasses [16-18]. Due to the purposeful engineering of nanoscale characteristics into the structure, nanostructured thin films and coatings

* Corresponding Author Email: dr.sami@uomustansiriyah.edu.iq

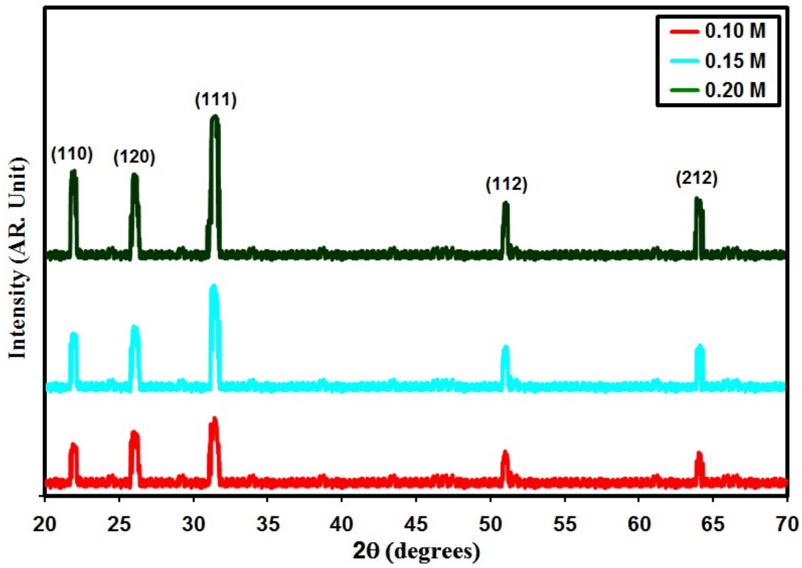

Fig. 1. XRD styles of the prepared films.

have characteristics that differ from homogeneous materials [19, 20].

Because of their prospective use in optoelectronic devices and solar cells, semiconductors from the IV-VI group have gotten a lot of interest [21, 22]. Due to its advantageous optical bandgap energy, high optical absorption coefficient, and high optical transmission, tin monosulfide (SnS) has attracted a lot of interest as an absorber layer in the production of photovoltaic systems in recent years within the IV-VI group [23-26]. Tin monosulfide is a p-type semiconductor made out of inexpensive and non-toxic materials. It may form cubic as well as orthorhombic crystal structures [27]. It has been reported to have a broad bandgap, ranging from 0.9 to 1.8 eV [28]. These attractive properties make it candidate for different application.

In this study, SnS thin film was prepared via CBD route. The structural and morphological properties of prepared thin film was studied via XRD, AFM, SEM, and UV-Vis analysis comprehensively.

MATERIALS AND METHODS

CBD was utilized to synthesize SnS thin films. The bath contained 0.1 M of ($SnCl_2.2H_2O$), 0.15 M (C_2H_5NS) and ($Na_3C_6H_5O_7$) (TSC), that is dissolved in deionized water by 50 ml . Various TSC mixture (0.10 M, 0.15 M, and 0.20 M) concentrations are prepared. Drop by drop aqueous ammonia is added to adjust the solution Ph to 5.8. At room temperature, the mixtures are stirred by a motorized magnetic stirrer. Previous film deposition, commercial microscopic glass slides are cleaned with acetone, methanol and deionized water. The deposition is done for 4 h at 80°C. Then, the substrates are removed from the beaker, washed with deionized water and naturally dried. The deposited films are homogeneous.

The structural properties of the SnS films were studied by XRD. AFM was employed to study the surface of the films. Then optical transmittance are recorded employing UV-Visible spectrophotometer.

RESULTS AND DISCUSSION

Fig. 1, represent XRD styles of SnS films that are grown through the use of TSC (0.10–0.20 M) various concentrations . All peaks of SnS thin films are matched orthorhombic structure. The dominant peak was (111) plane is actually agrees with (ICDD card no.: 39-0354) [29].

The crystallite size D is evaluated from the Debye Scherer's formula [30-33]:

$$D = \frac{0.9\lambda}{\beta cos\theta} \quad (1)$$

Where β shows (FWHM).

From Fig. 2, it is stated that there is an increase in the D value with the increase of the TSC concentrations. This is consistent with other results that are published [34]. Moreover, the increasing of the average crystalline size with the increase of the TSC concentration may be assigned

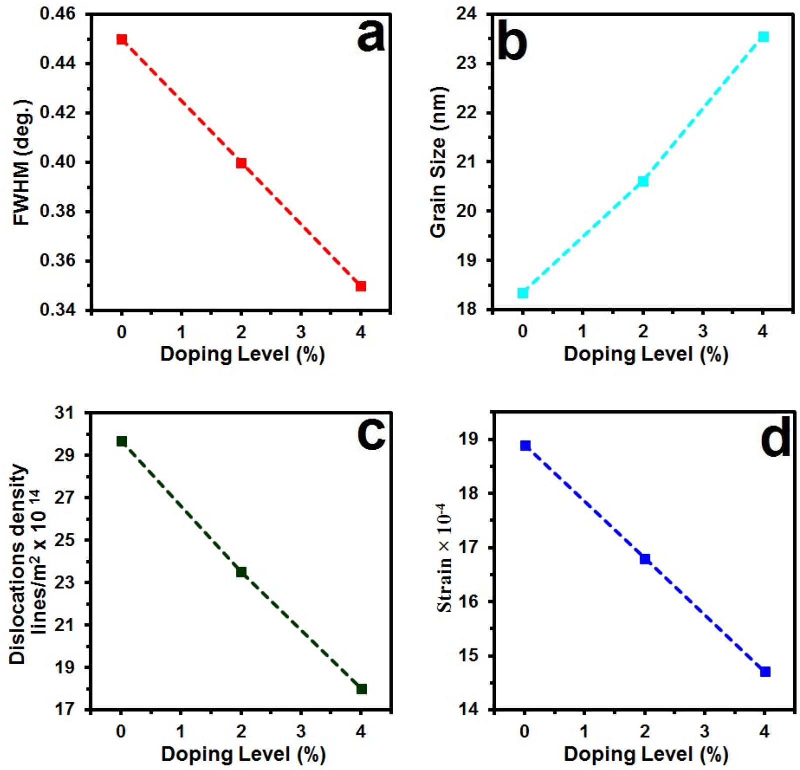

Fig. 2. FWHM (a) Grain size (b) Dislocation (c) Strain (d) of the prepared films.

Table 1. *D*, E_g and structural parameters of the prepared films.

TSC (M)	(hkl) Plane	2 θ (°)	FWHM (°)	Grain size (nm)	Optical bandgap (eV)	Dislocations density (× 10^{14})(lines/m^2)	Strain (× 10^{-4})
0.10	111	31.53	0.45	18.35	1.45	29.69	18.89
0.15	111	31.21	0.40	20.62	1.35	23.51	16.80
0.20	111	31.00	0.35	23.56	1.25	18.01	14.71

to the improvement of SnS crystallinity [35, 36].

The following equation estimate the dislocation density (*δ*) [37-40]:

$$\delta = \frac{1}{D^2} \qquad (2)$$

The following equation estimates the lattice strain (*ε*) [41-44]:

$$\varepsilon = \frac{\beta cos\theta}{4} \qquad (3)$$

The values of scrostrain in Table 1 offer an increase with increasing content of TSC. The

Calculated structural parameters are offered in Table. 1

The FWHM is represented in Fig. 2, Grain size, Dislocation density and Strain versus doping content. The inverse relationship between crystallite size and other parameters are noted in the Figure. Fig. 2 demonstrates β, D, δ and ε Strain versus doping.

The SnS thin film surface morphology is studied through the use of AFM, as it is shown in Fig. 3 which shows AFM measurement technique that offers the digital images that allow of surface features quantitative measurements such as root mean square (RMS) or average roughness R_a that are shown in the Table 2. When taking two images with dimensions, Fig. 3 (a_1, b_2 and c_1) 3D, it is noted that the films are regularly distributed in the small granules form connected without any spaces between them. Fig. 3 (a_2, b_2 and c_2) shows curved volumetric distribution for crystalline granules where difference with TSC content from 0.10 M to

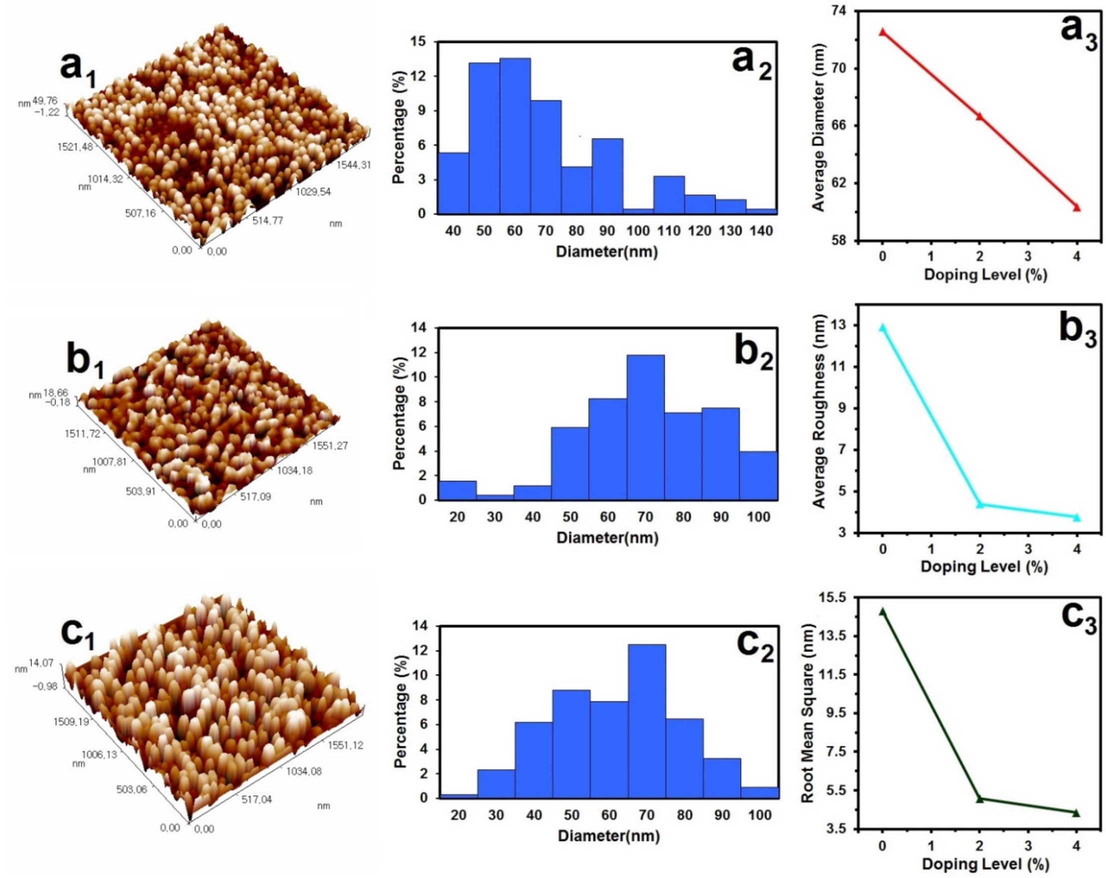

Fig. 3. AFM images of the prepared films (a_1, b_1 and c_1), granularly distributed (a_2, b_2 and c_2) and variation of AFM parameters via doping (a_3, b_3 and c_3).

Table 2. AFM parameters of the deposited films.

TSC (M)	Average Particle size nm	Roughness Average (nm)	R. M. S. (nm)
0.10	72.57	12.9	14.80
0.15	66.68	4.39	5.08
0.20	60.35	3.76	4.34

0.20 M respectively. From Fig. 3 (a_3, b_3 and c_3), Ra and RMS values of (12.90, 4.39 and 3.76) nm and (14.80, 5. 08 and 4.34) nm, respectively, The above analysis shows that TSC content affect the values of Ra and RMS. Table 2 represent the values of AFM parameters.

A sharp fall in transmittance at various wavelengths, which corresponds to absorption edge is shown in the recorded Optical transmittance spectra. From Fig. 4, it is proved that a TSC content from 0.10 M to 0.20 M respectively.

In general, from Fig. 4 it is observed that the optical transmittance is reduced from 95 to 80% with the increase of the TSC content from 0.10 M to 0.20 M. The transmittance shifts toward lower energies that join the content increment of TSC is explained by the fact that the increase of TSC from 0.20 M approaches the structure of bulk material [45]

The absorption coefficient (α) was specified by equation [46-49]:

$$\alpha = (2.303 \times A)/t \quad (4)$$

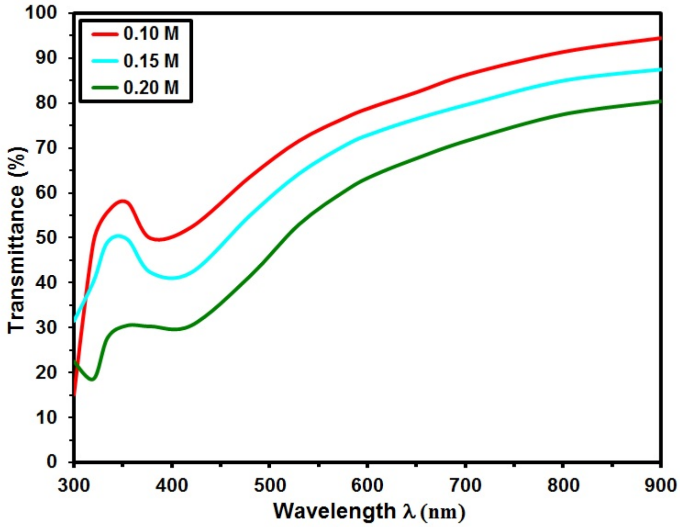

Fig. 4. Transmittance of the prepared films.

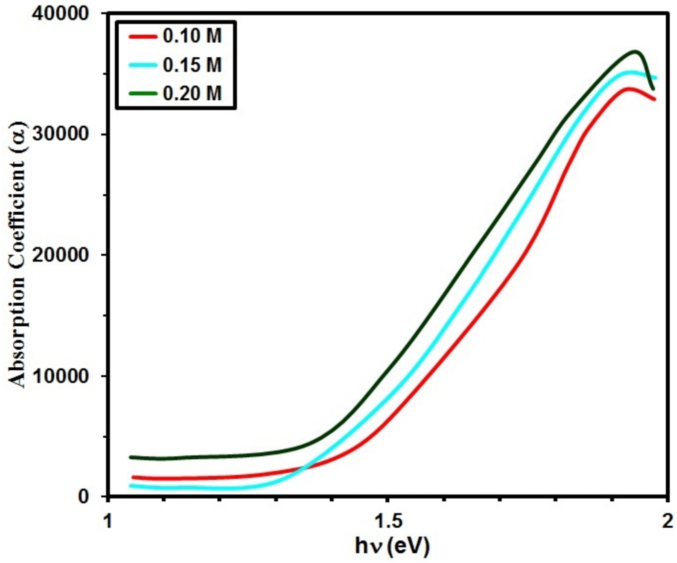

Fig. 5 α Vs hν of the prepared thin films.

Where (t) is film thickness, A is constant, Fig. 5. Shows α against the energy of photon (hυ) , it is observed that the films offers a high ($\alpha > 10^4 cm^{-1}$) which in turn shows direct transitions [50] .

Band gap variation was calculated from transmittance spectra and Tauc's formula [51-54]:

$$(\alpha h\nu) = A\left(h\nu - E_g\right)^{\frac{1}{2}} \qquad (5)$$

Where A is a constant, the relations are plotted between $(\alpha h\nu)^2$ and hν. From Fig. 6 we can conclude that the bandgap depends on the TSC content, E_g decreases as TSC concentration increases. The bandgap of nanocrystalline SnS films depends on the content of TSC from 0.10 M to 0.20 M its values were 1.45 and 1.25 eV, respectively [55].

Table 1 represent the values of bandgap.

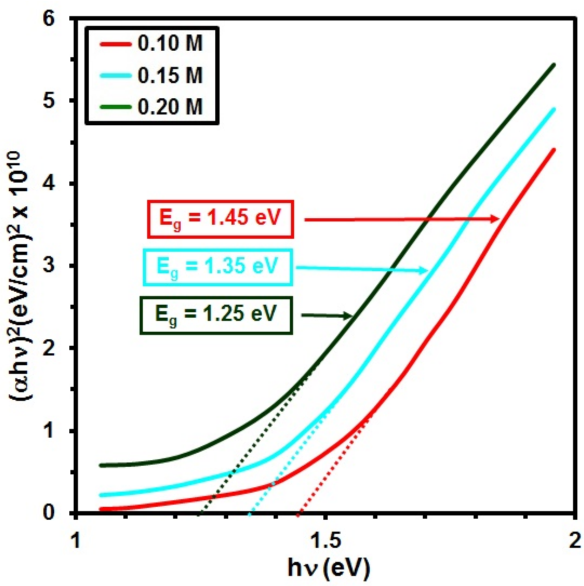

Fig. 6. $(\alpha h\nu)^2$ Vs hν of the prepared thin films.

CONCLUSION

The nanostructure tin sulfide films are produced successfully through CBD at 80 °C for 4 h through the use of various concentrations (0.10 M, 0.15 M and 0.20 M) of TSC. The orthorhombic structure of the grown SnS is revealed by the XRD spectra, as it is marked by the dominant peak of (111) plane. The results show that the increment of TSC content cause a decrement in crystalline size and a decrease in strain. The presence of the SnS phase in the deposited thin films decreased gradually with increasing TSC content. AFM image showed that the grain size of the nanoparticles observed in the range of 72.57 nm to 60.35 nm with TSC content, the optical transmittance exhibits excellent optical transparency. The optical transmittance reduced from 95 to 80%, with the increase of TSC content. The SnS films have ($\alpha > 10^4$ cm^{-1}). The energy bandgap range between 1.45 eV and 1.25 eV with the increase TSC content.

ACKNOWLEDGMENTS

Authors would appreciate Mustansiriyah University (www. uomustansiriyah.edu.iq) for supporting this work.

CONFLICT OF INTEREST

The authors declare that there is no conflict of interests regarding the publication of this manuscript.

REFERENCES

1. Liu W, Wang H. Flexible oxide epitaxial thin films for wearable electronics: Fabrication, physical properties, and applications. Journal of Materiomics. 2020;6(2):385-96.
2. Ma C, Wang M, Wang Z, Gao M, Wang J. Recent progress on thin film composite membranes for CO_2 separation. Journal of CO_2 Utilization. 2020;42:101296.
3. e Silva HdS, Marciano FR, de Menezes AS, Costa THdC, de Almeida LS, Rossino LS, et al. Morphological analysis of the TiN thin film deposited by CCPN technique. Journal of Materials Research and Technology. 2020;9(6):13945-55.
4. Chen X, Zhou Z, Lin Y-H, Nan C. Thermoelectric thin films: Promising strategies and related mechanism on boosting energy conversion performance. Journal of Materiomics. 2020;6(3):494-512.
5. Pedanekar RS, Shaikh SK, Rajpure KY. Thin film photocatalysis for environmental remediation: A status review. Current Applied Physics. 2020;20(8):931-52.
6. Xu W, Li H, Xu JB, Wang L. Recent advances of solution-processed metal oxide thin-film transistors. ACS applied materials & interfaces. 2018;10(31):25878-901.
7. Gour KS, Bhattacharyya B, Singh OP, Yadav AK, Husale S, Singh VN. Nanostructured Cu_2ZnSnS_4 (CZTS) thin film for self-powered broadband photodetection. Journal of Alloys and Compounds. 2018 ;735:285-90.
8. Weng Z, Ma S, Zhu H, Ye Z, Shu T, Zhou J, Wu X, Wu H. CdTe thin film solar cells with a SnTe buffer layer in back contact. Solar Energy Materials and Solar Cells. 2018;179:276-82.
9. Lavasani SA, Mirzaee O, Shokrollahi H, Moghadam AK, Salami M. Magnetic and morphological characterization of $Bi_2Fe_4O_9$ nanoparticles synthesized via a new reverse chemical co-precipitation method. Ceramics International. 2017;43(15):12120-5.
10. Xiao P, Dorey R. Nanostructured Thin Films and Coatings. Journal of Nanomaterials. 2008;2008:1-2.
11. Tiwari KJ, Vinod V, Subrahmanyam A, Malar P. Growth

and characterization of chalcostibite $CuSbSe_2$ thin films for photovoltaic application. Applied Surface Science. 2017 ;418:216-24.
12. Saksena S, Pandya DK, Chopra KL. Electroconversion of CdS to Cu_xS for thin film solar cells. Thin Solid Films. 1982;94(3):223-32.
13. Lokhande CD. Chemical deposition of metal chalcogenide thin films. Materials Chemistry and Physics. 1991;27(1):1-43.
14. Suehiro S, Kimura T, Yokoe D, Takahashi S. Synthesis of highly c-axis-oriented ZnO thin films using novel laser-enhanced electrospray CVD under atmospheric pressure. CrystEngComm. 2017;19(40):5995-6001.
15. Haidar F, Pradel A, Chen Y, Record M-C. Deposition of Sb_2Se_3 thin films on Pt substrate via electro-chemical atomic layer epitaxy (EC-ALE). Journal of Electroanalytical Chemistry. 2020;879:114774.
16. Thoka RW, Moloi SJ, Ray SC, Pong WF, Lin IN. Microstructure and electronic properties of ultra-nano-crystalline-diamond thin films. Journal of Electron Spectroscopy and Related Phenomena. 2020;242:146968.
17. Kalaev D, Tuller HL, Riess I. Measuring ionic mobility in mixed-ionic-electronic-conducting nano-dimensioned thin films at near ambient temperatures. Solid State Ionics. 2018;319:291-5.
18. Wang C, Zhao J, Ma C, Sun J, Tian L, Li X, Li F, Han X, Liu C, Shen C, Dong L. Detection of non-joint areas tiny strain and anti-interference voice recognition by micro-cracked metal thin film. Nano Energy. 2017;34:578-85.
19. Manthrammel MA, Ganesh V, Shkir M, Yahia IS, Alfaify S. Facile synthesis of La-doped CdS nanoparticles by microwave assisted co-precipitation technique for optoelectronic application. Materials Research Express. 2018;6(2):025022.
20. Betty CA, Sehra K, Barick KC, Choudhury S. Facile preparation of Silicon/ZnO thin film heterostructures and ultrasensitive toxic gas sensing at room temperature: Substrate dependence on specificity. Analytica chimica acta. 2018;1039:82-90.
21. Zhang C, Zhang J, Lin C, Dai S, Chen F. Improvement of third-order nonlinear properties in GeS_2–Sb_2S_3–CsCl chalcogenide glass ceramics embedded with CsCl nano-crystals. Ceramics International. 2020;46(18):27990-5.
22. Lu X, Zhang R, Zhang Y, Zhang S, Ren J, Strizik L, et al. Crystal-field engineering of ultrabroadband mid-infrared emission in Co^{2+}-doped nano-chalcogenide glass composites. Journal of the European Ceramic Society. 2020;40(1):103-7.
23. Bronusiene A, Popov A, Ivanauskas R, Ancutiene I. Preparation and characterization of tin sulfide films with or without sodium chloride. Chemical Physics. 2020;535:110766.
24. Choi J-W, Oh J, Ngoc Van TT, Kim J, Hwang H, Kim CG, et al. Tin oxysulfide composite thin films based on atomic layer deposition of tin sulfide and tin oxide using $Sn(dmamp)_2$ as Sn precursor. Ceramics International. 2020;46(4):5109-18.
25. Nefzi C, Souli M, Cuminal Y, Kamoun-Turki N. Effect of sulfur concentration on structural, optical and electrical properties of Cu_2FeSnS_4 thin films for solar cells and photocatalysis applications. Superlattices and Microstructures. 2018;124:17-29.
26. Arulanantham AMS, Valanarasu S, Jeyadheepan K, Kathalingam A. Effect of thermal annealing on nebulizer spray deposited tin sulfide thin films and their application in a transparent oxide/CdS/SnS heterostructure. Thin Solid Films. 2018;666:85-93.
27. Barman B, Bangera KV, Shivakumar GK. Evaluation of semiconducting p-type tin sulfide thin films for photodetector applications. Superlattices and Microstructures. 2019;133:106215.
28. Burton LA, Colombara D, Abellon RD, Grozema FC, Peter LM, Savenije TJ, et al. Synthesis, Characterization, and Electronic Structure of Single-Crystal SnS, Sn2S3, and SnS_2. Chemistry of Materials. 2013;25(24):4908-16.